Neighborhood Deprivation Shapes Motivational-Neurocircuit Recruitment in Children

Teagan S. Mullins[1,2], Ethan M. Campbell[1,2], and Jeremy Hogeveen[1,2]

[1]Department of Psychology, The University of New Mexico, and [2]Psychology Clinical Neurosciences Center, The University of New Mexico

Abstract

Implementing motivated behaviors on the basis of prior reward is central to adaptive human functioning, but aberrant reward-motivated behavior is a core feature of neuropsychiatric illness. Children from disadvantaged neighborhoods have decreased access to rewards, which may shape motivational neurocircuits and risk for psychopathology. Here, we leveraged the unprecedented neuroimaging data from the Adolescent Brain Cognitive Development (ABCD) study to test the hypothesis that neighborhood socioeconomic disadvantage shapes the functional recruitment of motivational neurocircuits in children. Specifically, via the ABCD study's monetary-incentive-delay task ($N = 6,396$ children; age: 9–10 years), we found that children from zip codes with a high Area Deprivation Index demonstrate blunted recruitment of striatum (dorsal and ventral nuclei) and pallidum during reward anticipation. In fact, blunted dorsal striatal recruitment during reward anticipation mediated the association between Area Deprivation Index and increased attention problems. These data reveal a candidate mechanism driving elevated risk for psychopathology in children from socioeconomically disadvantaged neighborhoods.

Keywords

socioeconomic status, reward processing, childhood, functional MRI, Adolescent Brain Cognitive Development Study, open data

Received 9/5/19; Revision accepted 2/29/20

Income inequality in the United States has risen dramatically in recent decades (Saez & Zucman, 2016). The mental health implications of this shift are significant; children from socioeconomically disadvantaged neighborhoods are at an increased risk for developing internalizing (e.g., Deng et al., 2006) and externalizing (e.g., Rowland et al., 2018) disorders. Given the established link between socioeconomic disadvantage and psychopathology, it is critical to better understand the neurodevelopmental mechanisms driving this association.

Making decisions on the basis of prior reward is central to shaping adaptive behavior. Socioeconomically disadvantaged youths grow up with diminished access to rewards and demonstrate structural aberrations in several subcortical structures that underlie reward-guided decision-making (Jenkins et al., 2020), and early life stress is associated with blunted ventral striatal recruitment during reward processing (Hanson et al., 2016). Similarly, children with internalizing and externalizing problems demonstrate aberrant dorsal and ventral striatal recruitment during reward processing (Bjork, Chen, Smith, & Hommer, 2010; Guyer et al., 2014). Importantly, relatively few studies have directly probed the impact of childhood socioeconomic disadvantage on brain function and, in turn, how aberrant neural recruitment during reward processing shapes risk for psychopathology in disadvantaged children.

The Adolescent Brain Cognitive Development (ABCD) study provides an unprecedented opportunity to specify the relationship among deprivation, psychopathology,

Corresponding Author:
Jeremy Hogeveen, The University of New Mexico, Department of Psychology, Logan Hall MSC03 2220, 1 University of New Mexico, Albuquerque, NM 87131
E-mail: jhogeveen@unm.edu

and motivational-neurocircuit neurodevelopment. A representative sample of children from the United States completed a battery of clinical, demographic, and functional neuroimaging assessments in the baseline ABCD visit (Garavan et al., 2018). Here, we leveraged ABCD's monetary-incentive-delay (MID) functional MRI (fMRI) task, which involves working to obtain rewards or avoid losses, is a robust activator of motivational neurocircuits (Knutson, Adams, Fong, & Hommer, 2001), and is sensitive to neurodevelopmental differences (Bjork, Smith, Chen, & Hommer, 2010). We also examined psychopathology measures (Child Behavior Checklist, or CBCL; Achenbach & Rescorla, 2001) and a measure of neighborhood deprivation via U.S. Census data (Area Deprivation Index, or ADI; standardized to 100 ± 20; higher numbers indicate greater deprivation; Kind et al., 2014). Our hypothesis was that ADI would be associated with blunted recruitment of motivational neurocircuits during reward processing, which was expected to mediate the association between ADI and psychopathology.

Method

Participants

After downloading the prepackaged baseline ABCD data set from the National Institute of Mental Health Data Archive, we filtered the data to include only participants who (a) completed the MID task, (b) had parent-reported CBCL scores available, (c) had a parent-reported zip code enabling the ADI calculation, and (d) were scanned on Siemens or GE scanners.[1] This led to the inclusion of 6,396 children (age: 9–10 years) in the current study. The sample size of the ABCD study was designed to be sufficient to detect small to medium effect sizes at the population level (Garavan et al., 2018).

The ABCD sample is socioeconomically diverse. In the current sample, 18% of children were from households with a combined annual income of less than $35,000 (51% female; 71% nonmarried parents; age: $M = 119.0$ months, $SD = 7.41$, $SEM = 0.22$; 49% non-White; ADI: $M = 106.3$, $SD = 14.0$, $SEM = 0.41$), 9% of children were from households with a combined annual income of $35,000 to $50,000 (53% female; 52% nonmarried parents; age: $M = 119.2$ months, $SD = 7.42$, $SEM = 0.32$; 36% non-White; ADI: $M = 102.7$, $SD = 14.9$, $SEM = 0.63$), 14% of children were from households with a combined annual income of $50,000 to $75,000 (48% female; 32% nonmarried parents; age: $M = 119.3$ months, $SD = 7.47$, $SEM = 0.25$; 20% non-White; ADI: $M = 99.9$, $SD = 14.9$, $SEM = 0.51$), 15% of children were from households with a combined annual income of $75,000 to $100,000 (51% female; 17% nonmarried parents; age: $M = 119.0$ months, $SD = 7.57$, $SEM = 0.24$; 14% non-White; ADI: $M = 96.4$, $SD = 15.6$, $SEM = 0.50$), 33% of children were from households with a combined annual income of $100,000 to $200,000 (48% female; 9% nonmarried parents; age: $M = 119.7$ months, $SD = 7.48$, $SEM = 0.16$; 11% non-White; ADI: $M = 90.1$, $SD = 17.3$, $SEM = 0.38$), and 12% of children were from households with a combined annual income of $200,000 or more (49% female; 5% nonmarried parents; age: $M = 119.9$ months, $SD = 7.39$, $SEM = 0.27$; 12% non-White; ADI: $M = 71.0$, $SD = 28.0$, $SEM = 1.04$). Child household income did not vary as a function of biological sex ($p = .247$) but differed significantly with respect to parent marital status ($p < .001$), age ($p = .003$), race ($p < .001$), and neighborhood deprivation (i.e., ADI; $p < .001$).

ABCD study procedure

MRI scanning. ABCD data collection took place at 21 sites across the United States on 3T MRI scanners (Siemens Prisma or GE MR750). Study site was included in all inferential analyses as a random effect in the current study to ensure that any explained variance was not confounded by scanner-specific variance. Participants completed both a T1-weighted anatomical MRI sequence—matrix = 256 × 256; slices = 176 (Siemens), 208 (GE); field of view = 256 × 256; resolution = 1-mm isotropic space; repetition time = 2,500 ms (Siemens, GE); echo time = 2.88 ms (Siemens), 2 ms (GE); flip angle = 8—and two multiband fMRI sequences for the MID task—matrix = 90 × 90, slices = 60, field of view = 216 × 216, resolution = 2.4-mm isotropic space, repetition time = 800 ms, echo time = 30 ms, flip angle = 52, multiband factor = 6 (Casey et al., 2018). Children completed motion-compliance training prior to the MRI scanning session in a mock MRI environment that involved motion-capture devices that presented feedback to the child. Prospective motion correction for the T1-weighted sequence involved the collection of brief head-tracking images embedded within the main sequence and compensation for head motion on the basis of those images (Hagler et al., 2019). Additionally, for fMRI data collected at all study sites using Siemens scanners, Framewise Integrated Real-Time MRI Monitoring software (Dosenbach et al., 2017) was used to track participants' head motion in real time, enabling scanner operators to correct motion by providing verbal feedback to participants or to collect additional data (Hagler et al., 2019). All scans were completed using standard adult-size multichannel head coils because the use of custom age-appropriate head coils would confound future longitudinal analyses of the ABCD study data. Stimuli for the MID task were presented using E-Prime Professional software (Version 2.0; Schneider, Eschman, & Zuccolotto, 2012), and responses were recorded with Current Designs button boxes (Science Plus Group, Groningen, The Netherlands).

Image preprocessing. The ABCD fMRI preprocessing and analysis stream is maintained by the ABCD Data Analysis and Informatics Center. Collectively, these scripts are referred to as the Multi-Modal Processing Stream (Hagler et al., 2019) and incorporate functions from open-source neuroimaging software packages (e.g., FreeSurfer: Fischl, 2012; the FMRIB Sofware Library (fsl.fmrib.ox.ac.uk); and Analysis of Functional NeuroImages: Cox, 1996). For a comprehensive description of the analysis pipeline, see Hagler et al. (2019). Briefly, analysis of the T1-weighted structural images involved a combination of gradient warp correction, bias field correction, and resampling to 1-mm isotropic space. Analysis of the fMRI data comprised motion correction, B0 distortion correction, gradient warp correction, and resampling to 2.4-mm isotropic space. For retrospective head-motion correction, the ABCD team regressed out variance associated with translational and rotational head movements and censored time points with framewise displacement above 0.9 mm (Hagler et al., 2019), and we included mean framewise displacement as a covariate in all group-level fMRI models.

MID task. Casey et al. (2018) provided full details on the MID task and all ABCD fMRI data-collection protocols. Each trial of the MID task starts with an incentive cue telling participants that they have a chance to win money (reward trial), have a chance to lose money (loss trial), or have no money at stake (neutral trial; Fig. 1b). Participants then make a speeded response to a target, titrated to ensure approximately 60% accuracy. If participants respond in time, they receive positive feedback (win money or avoid losing money); otherwise, they receive negative feedback (do not win money or lose money). As in the standard procedure for the MID task (Knutson et al., 2001), reward and loss trials randomly varied between small ($0.20) and large ($5.00) incentives. In total, the MID task contained 40 reward trials, 40 loss trials, and 20 neutral trials split evenly across two fMRI runs. Primary fMRI contrasts on the MID task are (a) reward anticipation versus neutral, (b) loss anticipation versus neutral, (c) reward positive versus negative feedback, and (d) loss positive versus negative feedback. The ABCD team also segmented participant-specific motivational-neurocircuit regions of interest (ROIs) via FreeSurfer (Fischl, 2012) and computed mean beta weights in our motivation-circuit ROIs during all four primary contrasts.

Child Behavior Checklist (CBCL). To assay psychopathology, we focused on parent-reported CBCL data from the Achenbach System of Empirically Based Assessment (ASEBA; Achenbach & Rescorla, 2001). We primarily focused on the ASEBA domains of internalizing and externalizing problems, which assay a set of issues commonly faced by children with developmental psychopathology. The internalizing-problems domain comprises three subdomains: anxious-depressed symptoms (e.g., "fears going to school"), withdrawn-depressed symptoms (e.g., "would rather be alone than with others"), and somatic complaints (e.g., "stomachaches"). The externalizing-problems domain of the ASEBA also comprises three subdomains: attention problems (characterized by both inattention, e.g., "can't concentrate, can't pay attention for long," and hyperactivity/impulsivity, e.g., "can't sit still, restless, or hyperactive"), aggression (e.g., "cruelty, bullying, or meanness to others"), and rule-breaking behaviors (e.g., "destroys things belonging to his/her family or others").

Current analysis

Local processing and analysis of ABCD data were performed using Python (Version 3.7.6; Python Core Team, 2019) and the R programming environment (Version 3.5.0; R Core Team, 2018). The code is provided in the Supplemental Material available online, and the results can be recreated by any researchers with authorization to download the ABCD data. In the current study, we focused on four ROIs from the MID-task data set: amygdala, ventral striatum (accumbens area), dorsal striatum (caudate and putamen), and pallidum (see Fig. 1a). Prior meta-analytic research has highlighted the selected ROIs as being critical to a network of subcortical structures that underlie reward processing throughout development (Silverman, Jedd, & Luciana, 2015). Furthermore, recent evidence has demonstrated structure variations in these ROIs based on socioeconomic disadvantage in youth (Jenkins et al., 2020). For the reward-anticipation-versus-neutral and loss-anticipation-versus-neutral models, we filtered out participants with beta weights in any of these ROIs 3 times the interquartile range, resulting in final samples of 6,235 for any analyses of the reward-anticipation-versus-neutral contrast, 6,238 for any analyses of the loss-anticipation-versus-neutral contrast, 6,160 for any analyses of the reward-positive-versus-negative-feedback contrast, and 6,153 for any analyses of the loss-positive-versus-negative-feedback contrast.

The current analysis proceeded in three phases. In Phase 1, we modeled psychopathology (CBCL-domain scores) as a function of neighborhood socioeconomic disadvantage (ADI). In Phase 2, we modeled MID-task fMRI activity (reward-anticipation-versus-neutral contrast, loss-anticipation-versus-neutral contrast, reward-positive-versus-negative-feedback contrast, and loss-positive-versus-negative-feedback contrast) within our a priori ROIs as a function of ADI. Importantly, all models were fitted first with household ADI as a single fixed effect and then in a linear mixed-effects model covarying for potential confounds including five fixed effects (age in months, biological sex, race, parents' marital status, and

a

b
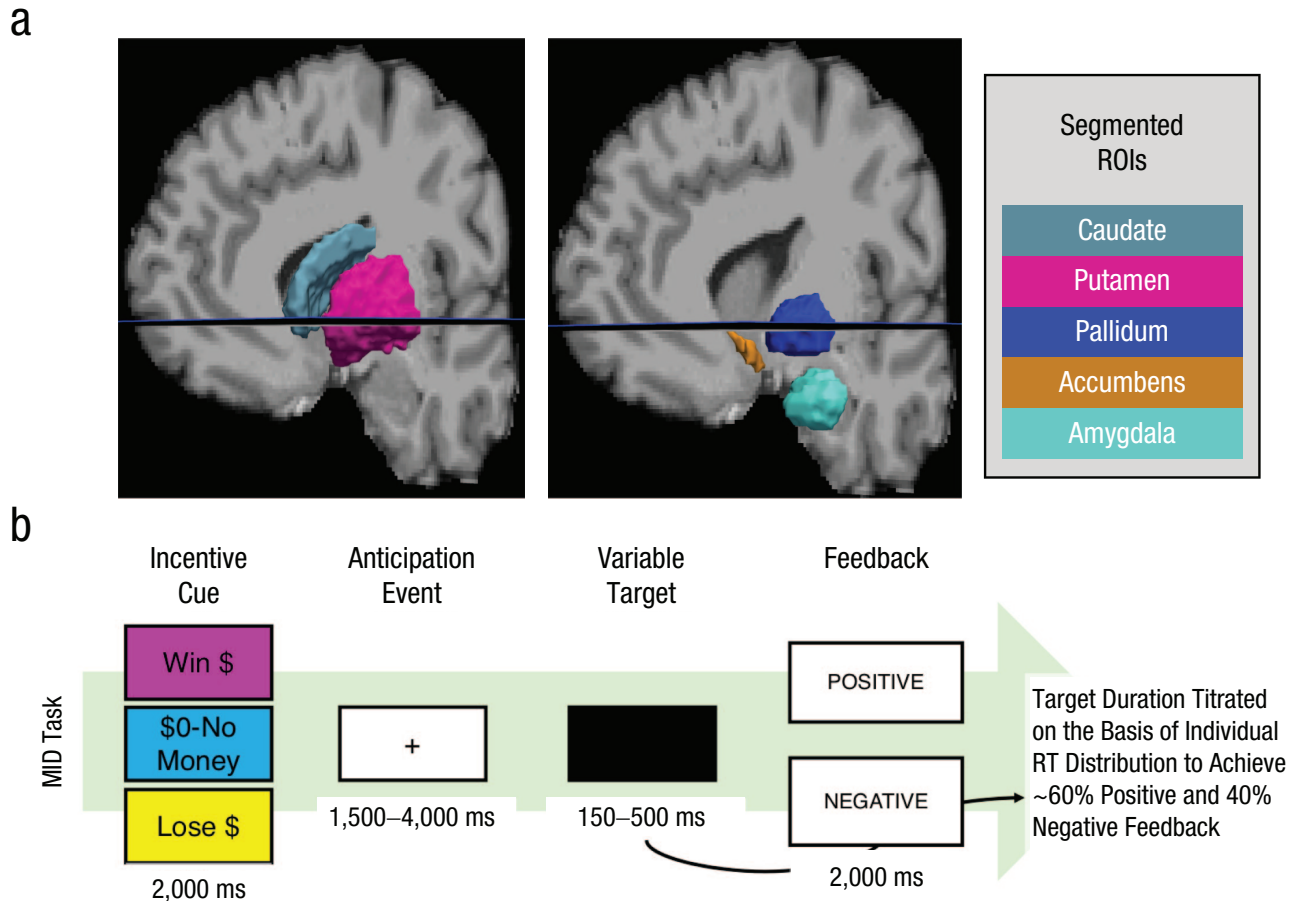
Fig. 1. Regions of interest and the experimental task. The brain images (a) show a sample participant's subcortical region-of-interest segmentation (obtained using FreeSurfer; Fischl, 2012). In the current study, dorsal striatum refers to both caudate and putamen, and ventral striatum refers to the accumbens area. The schematic (b) shows the sequence of events in the monetary-incentive-delay (MID) task used in the Adolescent Brain Cognitive Development study (Casey et al., 2018), which is titrated to ensure approximately 60% accuracy.

framewise displacement for fMRI models) and one random effect (ABCD study site). This was done to minimize the variance explained by these confounds, given that children from different socioeconomic backgrounds have distinct demographic features. If ADI did not have a statistically significant effect on a given outcome variable in the univariate model, we did not proceed to the mixed-effects model. Lastly, in Phase 3, we investigated the potential mediating relationship of motivational-neurocircuit recruitment on the association between ADI and psychopathology. First, we generated correlation matrices of all the variables in the current study (ADI, CBCL-subdomain scores, and MID-task motivational-neurocircuit activations). Next, for any ROI in which motivational-neurocircuit activation was correlated with both ADI and CBCL scores, we constructed mediation models using 1,000 bootstrapped samples to test for statistically significant direct and indirect effects. Notably, a false-discovery-rate (FDR) procedure was used to correct for multiple comparisons in each phase of the analysis pipeline ($q < 0.05$).

Results

Association between neighborhood deprivation and psychopathology

We modeled the CBCL internalizing and externalizing domains as a function of household ADI, both with and without covarying for potential confounding variables. An FDR correction was applied at each step. These models suggested that both externalizing and internalizing problems were higher in children from socioeconomically disadvantaged neighborhoods (i.e., had higher ADI scores), externalizing: $b = 0.047$, $SE = 0.006$, $t(6233) = 7.59$, $q < 7.56\mathrm{e}{-14}$; internalizing: $b = 0.030$, $SE = 0.006$, $t(6233) = 4.67$, $q = 3.06\mathrm{e}{-06}$. These effects remained significant after covarying for race, parents' marital status, and study site (externalizing: $b = 0.037$, $SE = 0.008$, $q < 5.28\mathrm{e}{-6}$; internalizing: $b = 0.023$, $SE = 0.008$, $q = 0.005$). Notably, age and sex were not included as covariates, given that the CBCL dependent measures had already been age- and gender-normalized

(Achenbach & Rescorla, 2001). Full-model parameter estimates and inferential results for the mixed-effects models are provided in Table S1 in the Supplemental Material. In sum, increased neighborhood-area deprivation was associated with elevated levels of developmental psychopathology in children from the ABCD study.

Association between neighborhood deprivation and MID-task neural activity

Reward-anticipation-versus-neutral contrast. We modeled mean beta weights during reward anticipation within eight a priori subcortical ROIs that are pivotal to motivated behavior—namely, amygdala, ventral striatum, dorsal striatum, and pallidum (left and right hemispheres)—as a function of household ADI. As in the CBCL analyses, models were fitted with household ADI as a direct fixed effect and then with several potentially confounding mixed effects included as covariates. Further, we applied an FDR correction for multiple comparisons across ROIs at each level. Household ADI did not predict amygdala recruitment in either hemisphere (left: $q = 0.464$; right: $q = 0.482$). Conversely, household ADI was associated with decreased ventral striatal activation—left: $b = -0.0003$, $SE = 0.0001$, $t(6174) = -2.27$, $q = 0.03$; right: $b = -0.0003$, $SE = 0.0001$, $t(6174) = -2.83$, $q = 0.009$—dorsal striatal activation—left: $b = -0.0004$, $SE = 0.0001$, $t(6174) = -4.06$, $q = 0.0002$; right: $b = -0.0005$, $SE = 0.0001$, $t(6174) = -4.44$, $q = 0.00007$—and pallidum activation—left: $b = -0.0002$, $SE = 0.00009$, $t(6174) = -2.23$, $q = 0.03$; right: $b = -0.0003$, $SE = 0.00009$, $t(6174) = -3.70$, $q = 0.0006$—during reward anticipation relative to neutral trials. The effects of ADI on bilateral dorsal striatal recruitment—left: $b = -0.0004$, $SE = 0.0001$, $t(6174) = -3.17$, $q = 0.006$; right: $b = -0.0004$, $SE = 0.0001$, $t(6174) = -3.62$, $q = 0.003$—right ventral striatal recruitment—$b = -0.0004$, $SE = 0.0001$, $t(6174) = -2.43$, $q = 0.032$—and right pallidum recruitment—$b = -0.0003$, $SE = 0.0001$, $t(6174) = -2.86$, $q = 0.012$—were robust to the inclusion of age, sex, marital status, framewise displacement, and study site as covariates (Fig. 2a). Left ventral striatum ($q = 0.144$) and pallidum ($q = 0.271$) were no longer associated with ADI after the covariates were fitted. Full-model parameter estimates and inferential results for the mixed-effects models are provided in Tables S2 to S5 in the Supplemental Material. In sum, higher neighborhood deprivation predicts blunted recruitment of motivational neurocircuits—particularly in the right hemisphere—during reward anticipation relative to neutral trials.

Loss-anticipation-versus-neutral and feedback contrasts. Beta weights from our a priori ROIs during loss anticipation were modeled as a function of household ADI. Household ADI did not significantly predict recruitment of any motivational-neurocircuit ROIs in the loss-anticipation-versus-neutral contrast (all qs ≥ 0.110). We ran additional analyses of motivational-neurocircuit recruitment during the feedback epoch, contrasting reward positive versus negative feedback and loss positive versus negative feedback. Household ADI significantly predicted increased bilateral amygdala recruitment in the reward-positive-versus-negative-feedback contrast—left: $b = 0.0004$, $SE = 0.0001$, $t(6176) = 3.23$, $q = 0.010$; right: $b = 0.0004$, $SE = 0.0001$, $t(6176) = 2.56$, $q = 0.041$—but these effects were not significant when analyses covaried for age, sex, parent marital status, framewise displacement, and study site (all qs $= 0.364$). ADI did not predict reward-positive-versus-negative-feedback contrast beta weights in any of the other ROIs (all qs ≥ 0.232), nor did it predict loss-positive-versus-negative-feedback contrast beta weights in any ROIs (all qs ≥ 0.308). Therefore, the observed effects of household ADI on motivational-neurocircuit recruitment seem to be selectively associated with reward anticipation, with no robust effects observed in the loss-anticipation or incentive-feedback contrasts.

Reaction time (RT) controls. It is possible that household ADI was associated with RTs during reward anticipation, which might have impacted its association with motivational-neurocircuit recruitment. We addressed this potential confound in two ways. First, we observed that although household ADI was associated with decreased RTs during reward trials—$b = -0.360$, $SE = 0.025$, $t(6174) = -14.2$, $p < 2.0e{-16}$—this effect was not robust to modeling the same confound variables that were included as covariates in the reward-anticipation-versus-neutral fMRI models ($p = .114$; Table S6 in the Supplemental Material). Second, given that our fMRI contrasts examined the difference between motivational-neurocircuit recruitment on reward-anticipation-versus-neutral trials, we ran additional models on the effect of ADI on the reward-anticipation-versus-neutral trial RT ratio: reward-anticipation-versus-neutral RT = (reward RT − neutral RT)/(reward RT + neutral RT). Modeling reward-anticipation-versus-neutral RT with an isolated fixed effect of household ADI did not yield a significant association between these variables ($p = .747$). Therefore, it does not appear that RTs—either during reward anticipation in isolation or during reward anticipation relative to neutral trials—were unexpectedly confounding the observed effects of ADI on motivational-neurocircuit recruitment during reward anticipation.

Neural mediation of the link between neighborhood deprivation and psychopathology

We generated a correlation matrix comprising ADI (after regressing out the potential confound variables included in our fMRI models), CBCL-subdomain scores

a

Reward-Anticipation-Versus-Neutral Contrast
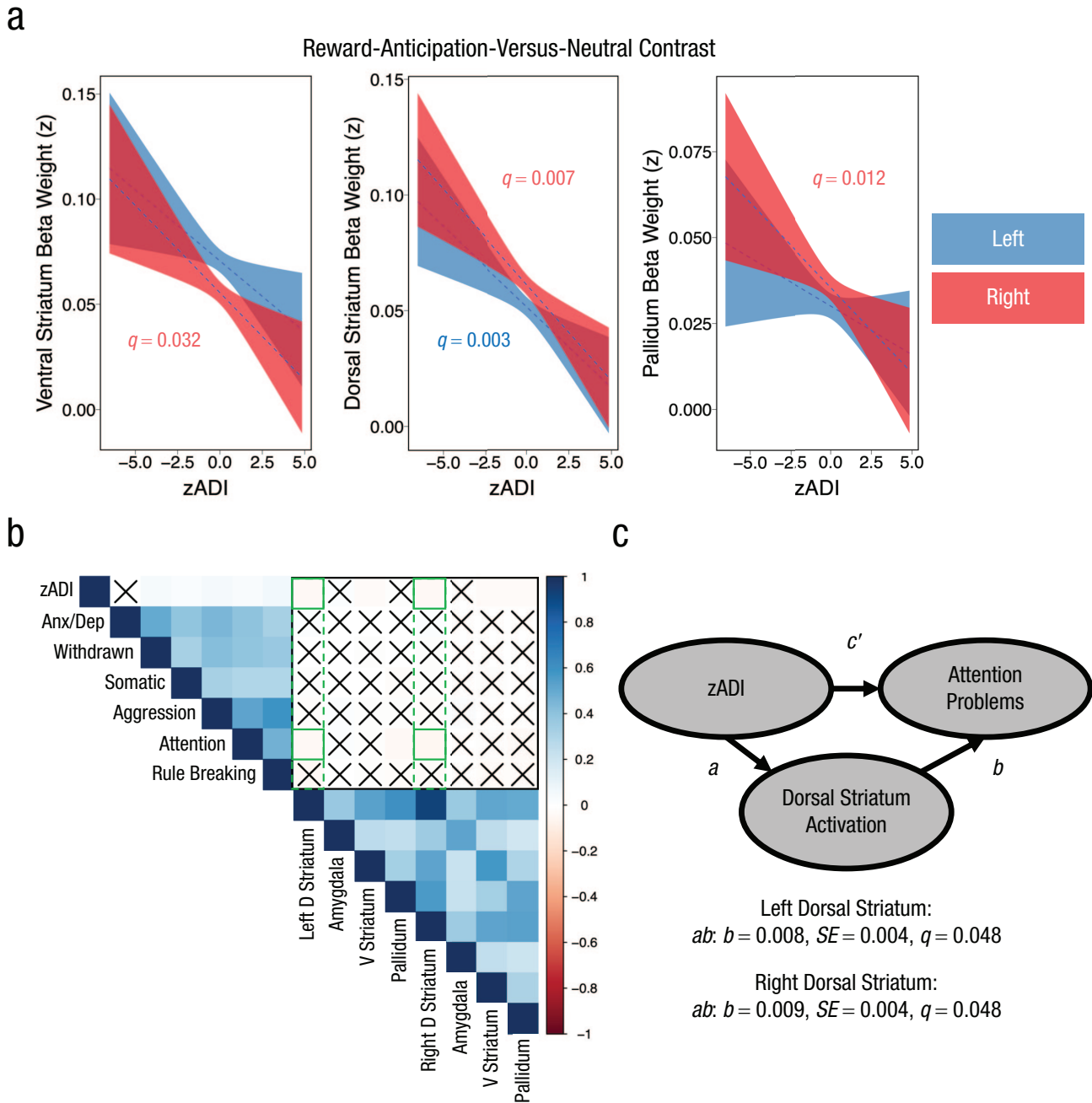
Fig. 2. Results for the reward-anticipation-versus-neutral contrast. The plots (a) show activation of ventral striatum, dorsal striatum, and pallidum, respectively, during the reward-anticipation-versus-neutral contrast as a function of Area Deprivation Index (ADI) after covarying for race, biological sex, parent marital status, age, framewise displacement, and study site (zADI). The correlation matrix (b) shows associations among zADI scores, brain regions activated in the reward-anticipation-versus-neutral contrast, and scores on the Child Behavior Checklist (CBCL). The CBCL measured anxiety/depression (Anx/Dep), withdrawn-depressed symptoms (Withdrawn), somatic complaints, aggression, and rule breaking. "X" indicates a nonsignificant correlation; green outlines appear where we observed evidence for a three-way relationship among ADI, CBCL, and monetary-incentive-delay task neural recruitment. The mediation model (c) shows the influence of covariate-adjusted ADI scores on attention problems, as mediated by dorsal striatum activity in the reward-anticipation-versus-neutral contrast. D Striatum = dorsal striatum; V Striatum = ventral striatum.

(anxiety/depression, withdrawn, somatic complaints, aggression, attention problems, and rule breaking), and reward-anticipation-versus-neutral neural recruitment. This correlation matrix suggested that bilateral dorsal striatum recruitment during reward anticipation was associated with both household ADI and CBCL attention problems (Fig. 2b). On the basis of our a priori interest in examining the mechanisms driving the

association between socioeconomic disadvantage and psychopathology, we fitted mediation models examining whether dorsal striatum recruitment during reward anticipation mediates the association between ADI and attention problems to probe this three-way relationship. These models were subjected to an FDR correction. The results indicated that bilateral dorsal striatum recruitment significantly mediated the association between ADI and attention-problems subdomain scores—left: *ab: b* = 0.008, *SE* = 0.004, *z* = 1.98, *q* = 0.048; right: *ab: b* = 0.009, *SE* = 0.004, *z* = 2.19, *q* = 0.048 (Fig. 2c; Table S7 in the Supplemental Material).

Discussion

These data suggest that neighborhood deprivation is associated with decreased recruitment of motivational neurocircuits—dorsal and ventral striatum as well as pallidum—during reward anticipation. Of particular relevance to public health, dorsal striatum activation during reward anticipation mediated the association between deprivation and attention problems in children. Previous studies have found aberrant dorsal striatal morphology in children with attention-deficit/hyperactivity disorder extending into adolescence (Shaw et al., 2014), suggesting that it will be critical to track longitudinal changes in dorsal striatum recruitment during reward processing and attention problems via future ABCD time points. Impaired reward-motivated behavior and attention problems can have devastating consequences as children progress through adolescence and adulthood (e.g., criminality, substance misuse), and specifying the mechanisms driving this relationship is a critical topic for facilitating evidence-based intervention.

More than any other ROI, dorsal striatum was impacted by neighborhood deprivation and mediated its relationship to externalizing. Whereas ventral striatum has been implicated in goal-directed reward learning, dorsal striatum has been implicated in action-outcome habitual learning (Balleine & O'Doherty, 2010). This suggests that interventions to reduce externalizing in children from deprived neighborhoods would do well to focus on shaping the environment to set up the child for success, rather than providing, for example, verbal instruction to change goal-directed behavior. Continued research on the neurobiological effects of neighborhood deprivation across adolescence (via ABCD) could be essential in informing the design of such interventions.

Three limitations should be noted. First, we leveraged mean beta weights in a priori ROIs to define motivational-neurocircuit activation. This may cause Type II errors if sub-ROI clusters wash out in the average or if unanalyzed ROIs were impacted by deprivation. In future studies, researchers should conduct whole-brain voxel-wise analysis of the ABCD MID-task data to determine whether ROIs beyond the scope of the current study are impacted by neighborhood deprivation. Second, parent-reported measures of internalizing in children are influenced by rater bias (Youngstrom, Loeber, & Stouthamer-Loeber, 2000), which may be the reason that we did not detect a relationship between MID-task striatal recruitment and internalizing subdomains (Knutson, Bhanji, Cooney, Atlas, & Gotlib, 2008). Third, these findings do not allow us to determine whether neighborhood deprivation modulates striatal activation to cause externalizing or whether a hidden variable associated with deprivation causes externalizing and, over time, leads to blunted striatal activation. Longitudinal analyses are needed to establish the temporal priority of these effects in order to test the hypothesis that blunted dorsal striatal activation causes increased attention problems in socioeconomically disadvantaged children.

ORCID iD

Jeremy Hogeveen (iD) https://orcid.org/0000-0001-9612-2085

Supplemental Material

Additional supporting information can be found at http:// journals.sagepub.com/doi/suppl/10.1177/0956797620929299

Note

1. A total of 879 participants who met other criteria were scanned on Philips scanners and excluded because of an ABCD study fMRI processing issue (https://github.com/ABCD-STUDY/ fMRI-cleanup).

References

Achenbach, T. M., & Rescorla, L. (2001). *Manual for the ASEBA school-age forms and profiles: An integrated system of multi-informant assessment.* Burlington, VT: Research Center for Children, Youth, and Families.

Balleine, B. W., & O'Doherty, J. P. (2010). Human and rodent homologies in action control: Corticostriatal determinants of goal-directed and habitual action. *Neuropsychopharmacology*, *35*, 48–69. doi:10.1038/npp.2009.131

Bjork, J. M., Chen, G., Smith, A. R., & Hommer, D. W. (2010). Incentive-elicited mesolimbic activation and externalizing symptomatology in adolescents. *The Journal of Child Psychology and Psychiatry*, *51*, 827–837. doi:10.1111/ j.1469-7610.2009.02201.x

Bjork, J. M., Smith, A. R., Chen, G., & Hommer, D. W. (2010). Adolescents, adults and rewards: Comparing motivational neurocircuitry recruitment using fMRI. *PLOS ONE*, *5*(7), Article e11440. doi:10.1371/journal.pone.0011440

Casey, B. J., Cannonier, T., Conley, M. I., Cohen, A. O., Barch, D. M., Heitzeg, M. M., . . . Dale, A. M. (2018). The Adolescent Brain Cognitive Development (ABCD) study: Imaging acquisition across 21 sites. *Developmental Cognitive Neuroscience*, *32*, 43–54. doi:10.1016/j.dcn.2018.03.001

Cox, R. W. (1996). AFNI: Software for analysis and visualization of functional magnetic resonance neuroimages. *Computers and Biomedical Research*, *29*, 162–173.

Deng, S., Lopez, V., Roosa, M. W., Ryu, E., Burrell, G. L., Tein, J.-Y., & Crowder, S. (2006). Family processes mediating the relationship of neighborhood disadvantage to early adolescent internalizing problems. *The Journal of Early Adolescence*, *26*, 206–231. doi:10.1177/0272431605285720

Dosenbach, N. U. F., Koller, J. M., Earl, E. A., Miranda-Dominguez, O., Klein, R. L., Van, A. N., . . . Fair, D. A. (2017). Real-time motion analytics during brain MRI improve data quality and reduce costs. *NeuroImage*, *161*, 80–93.

Fischl, B. (2012). FreeSurfer. *NeuroImage*, *62*, 774–781. doi:10.1016/j.neuroimage.2012.01.021

Garavan, H., Bartsch, H., Conway, K., Decastro, A., Goldstein, R. Z., Heeringa, S., . . . Zahs, D. (2018). Recruiting the ABCD sample: Design considerations and procedures. *Developmental Cognitive Neuroscience*, *32*, 16–22. doi:10.1016/j.dcn.2018.04.004

Guyer, A. E., Benson, B., Choate, V. R., Bar-Haim, Y., Perez-Edgar, K., Jarcho, J. M., . . . Nelson, E. E. (2014). Lasting associations between early-childhood temperament and late-adolescent reward-circuitry response to peer feedback. *Development and Psychopathology*, *26*, 229–243. doi:10.1017/S0954579413000941

Hagler, D. J., Hatton, S. N., Cornejo, M. D., Makowski, C., Fair, D. A., Dick, A. S., . . . Dale, A. M. (2019). Image processing and analysis methods for the Adolescent Brain Cognitive Development study. *NeuroImage*, *202*, Article 116091. doi:10.1016/j.neuroimage.2019.116091

Hanson, J. L., Albert, D., Iselin, A.-M. R., Carré, J. M., Dodge, K. A., & Hariri, A. R. (2016). Cumulative stress in childhood is associated with blunted reward-related brain activity in adulthood. *Social Cognitive and Affective Neuroscience*, *11*, 405–412. doi:10.1093/scan/nsv124

Jenkins, L. M., Chiang, J. J., Vause, K., Hoffer, L., Alpert, K., Parrish, T. B., . . . Miller, G. E. (2020). Subcortical structural variations associated with low socioeconomic status in adolescents. *Human Brain Mapping*, *41*, 162–171. doi:10.1002/hbm.24796

Kind, A. J. H., Jencks, S., Brock, J., Yu, M., Bartels, C., Ehlenbach, W., . . . Smith, M. (2014). Neighborhood socioeconomic disadvantage and 30-day rehospitalization: A retrospective cohort study. *Annals of Internal Medicine*, *161*, 765–774. doi:10.7326/M13-2946

Knutson, B., Adams, C. M., Fong, G. W., & Hommer, D. (2001). Anticipation of increasing monetary reward selectively recruits nucleus accumbens. *The Journal of Neuroscience*, *21*(16), Article RC159. doi:10.1523/JNEUROSCI.21-16-j0002.2001

Knutson, B., Bhanji, J. P., Cooney, R. E., Atlas, L. Y., & Gotlib, I. H. (2008). Neural responses to monetary incentives in major depression. *Biological Psychiatry*, *63*, 686–692. doi:10.1016/j.biopsych.2007.07.023

Python Core Team. (2019). *Python: A dynamic, open source programming language*. Retrieved from https://www .python.org/psf/

R Core Team. (2018). R: *A language and environment for statistical computing*. Retrieved from http://www.R-project .org

Rowland, A. S., Skipper, B. J., Rabiner, D. L., Qeadan, F., Campbell, R. A., Naftel, A. J., & Umbach, D. M. (2018). Attention-deficit/hyperactivity disorder (ADHD): Interaction

between socioeconomic status and parental history of ADHD determines prevalence. *Journal of Child Psychology and Psychiatry*, *59*, 213–222. doi:10.1111/jcpp.12775

Saez, E., & Zucman, G. (2016). Wealth inequality in the United States since 1913: Evidence from capitalized income tax data. *The Quarterly Journal of Economics*, *131*, 519–578. doi:10.1093/qje/qjw004

Schneider, W., Eschman, A., & Zuccolotto, A. (2012). *E-Prime 2.0 reference guide manual*. Pittsburgh, PA: Psychology Software Tools.

Shaw, P., De Rossi, P., Watson, B., Wharton, A., Greenstein, D., Raznahan, A., . . . Chakravarty, M. M. (2014). Mapping the development of the basal ganglia in children with attention-deficit/hyperactivity disorder. *Journal of the American Academy of Child & Adolescent Psychiatry*, *53*, 780–789.e11. doi:10.1016/j.jaac.2014.05.003

Silverman, M. H., Jedd, K., & Luciana, M. (2015). Neural networks involved in adolescent reward processing: An activation likelihood estimation meta-analysis of functional neuroimaging studies. *NeuroImage*, *122*, 427–439. doi:10.1016/j.neuroimage.2015.07.083

Youngstrom, E., Loeber, R., & Stouthamer-Loeber, M. (2000). Patterns and correlates of agreement between parent, teacher, and male adolescent ratings of externalizing and internalizing problems. *Journal of Consulting and Clinical Psychology*, *68*, 1038–1050. doi:10.1037/0022-006X.68.6.1038